www.ietdl.org

Published in IET Communications
Received on 27th June 2010
Revised on 22nd October 2010
doi: 10.1049/iet-com.2010.0528

ISSN 1751-8628

Blind timing and carrier synchronisation in distributed multiple input multiple output communication systems

A.A. Nasir S. Durrani R.A. Kennedy

School of Engineering, College of Engineering and Computer Science, The Australian National University, Canberra, Australia
E-mail: ali.nasir@anu.edu.au

Abstract: This study addresses the problem of joint blind timing and carrier synchronisation in a (distributed-M) $\times$ N antenna system where the objective is to estimate the M carrier offsets, the M timing offsets and to recover the transmitted symbols for each of the M users given only the measured signal at the N antennas of the receiver. The authors propose a modular receiver structure that exploits blind source separation to reduce the problem into more tractable sub-problems of estimating individual timing and carrier offsets for multiple users. This leads to a robust solution of low complexity. The authors investigate the performance of the estimators analytically using modified Cramer–Rao bounds and computer simulations. The results show that the proposed receiver exhibits robust performance over a wide range of parameter values, even with worst-case Doppler of 200–300 Hz and frame size as small as 400 symbols. This work is relevant to future wireless networks and is a complete solution to the problem of estimating multiple timing and carrier offsets in distributed multiple input multiple output (MIMO) communication systems.

1 Introduction

It is well known that multiple input multiple output (MIMO) systems can be utilised to achieve a multiplexing gain, a diversity gain or an antenna gain, thus enhancing the bit rate, the error performance or the signal-to-noise-plus-interference ratio, respectively, of wireless systems [1, 2]. However, cost, size and power consumption issues limit the applicability of large antenna arrays for mobile devices in wireless networks. Thus, the concept of distributed MIMO systems has been proposed, especially in the context of future wireless networks, where individual users can pool their antenna resources to form virtual MIMO systems to transmit information to a common destination [3, 4]. A fundamental requirement, underlying this paradigm, is the need to achieve timing and carrier synchronisation for all the distributed users. It has been shown that if the synchronisation errors are large, the performance of distributed MIMO systems is hugely degraded [5–7]. These results demonstrate the need for developing accurate timing and carrier synchronisation methods in distributed MIMO systems.

The fundamental problem of synchronisation in distributed MIMO systems is generally more difficult and complex than in conventional MIMO systems. In a conventional MIMO system with collocated antennas or a single user MIMO system, all the transmitters are physically connected to the same oscillator and hence there is only a single frequency offset and a single timing offset that needs to be estimated [8, 9]. However, in a distributed MIMO system, a mismatch between each of the transmitter and receiver oscillators results in multiple carrier frequency offsets at the destination node. Similarly, there are multiple timing offsets because of independent timing references between the transmitter and receiver clocks and unequal transmitter and receiver distances on the distributed links. In addition, as the number of users increases, the estimation problem becomes even more challenging as the number of unknowns also increases.

Recently, a limited number of papers have looked at the problem of estimating either multiple timing offsets or multiple carrier offsets. A pilot-based timing synchronisation scheme for sensor networks (with multiple static nodes) is presented in [10]. A timing synchronisation scheme in decode and forward cooperative communication systems is proposed in [11], but it requires the use of pilot sequences. A blind method of multiple carrier frequency offset estimation is proposed in [12], but it requires phase-locked loops. Training-based schemes, while computationally attractive, are bandwidth consuming and their use may sometimes become unrealistic or impractical. For instance, no training signal may be available to receivers in military communication scenarios and defence applications. In a broadcast scenario in a wireless communication network, it is highly undesirable for the transmitter to engage in a training session for a single user by temporarily suspending its normal transmission to a number of other users. On the other hand, blind synchronisation techniques are well motivated because of the lack of centralised coordination available in distributed

© The Institution of Engineering and Technology 2011

communication systems. The existing literature on blind estimation of multiple timing and carrier offsets is rather sparse. To the best of author's knowledge, the problem of estimating multiple timing and carrier offsets in distributed MIMO communication systems has not been considered in any existing literature.

In this paper, we present a receiver architecture for blind timing and carrier synchronisation in distributed MIMO systems, where M users send independent information to a destination equipped with N multiple antennas. Our approach is based on the principle of decoupling of the timing and carrier offsets from user to user. This in turn allows us to use efficient existing techniques to accurately estimate these multiple parameters. The proposed approach provides an appealing, low-complexity alternative to the complex and difficult problem of joint estimation of multiple timing and carrier offsets. The major contributions of this paper are listed below:

- We recast the blind MIMO system identification technique in [13] in a distributed MIMO communication scenario to enable decoupling of the timing and carrier offsets from user to user. This breaks up the overall complex problem of jointly estimating multiple timing and carrier offsets into more tractable sub-problems of estimating individual timing and carrier offsets for multiple users.
- We propose a novel modular receiver structure. The receiver model encompasses the following, quite different, computational techniques: (i) the blind source separation technique in [13] as it can effectively separate the users under reasonable timing and carrier offsets, (ii) the blind carrier estimation technique in [14] as it works well in the presence of timing offsets and finally (iii) the blind timing offset estimation technique in [15].
- We show that the proposed blind receiver exhibits robust performance under a wide range of parameter values. For independent and identically distributed (i.i.d.) channel model, increasing the frame size D leads to better estimation of frequency and timing offsets and improves the system bit error rate (BER) performance. For Rayleigh fading channel model, larger frame sizes can degrade performance because of the decorrelation effect of the channel. In addition, for a (distributed-M) $\times N$ system, $N = M + 1$ antenna receiver yields close to best performance. Increasing N further results in diminishing returns. Overall, the proposed receiver yields satisfactory results even with worst-case Doppler of 200–300 Hz and frame size as small as 400 symbols.

The rest of this paper is organised as follows. The existing relevant literature from conventional MIMO systems, for blind channel estimation and synchronisation, is summarised in Section 2. The mathematical system model and problem statement is provided in Section 3. The proposed blind receiver architecture is presented in Section 4. The performance of our estimators is analysed in Section 5. In Section 6, simulation results demonstrate the acceptable performance of our proposed method. Finally, the conclusions are drawn in Section 7.

Notation: Superscripts $(\cdot)^*$, $(\cdot)^{\mathrm{H}}$ and $(\cdot)^{\mathrm{T}}$ denote the conjugate, the conjugate transpose and the transpose operators, respectively. $|\cdot|$ is the modulus operator and $E\{\cdot\}$ represents the expected value for the corresponding signal or sequence. Notations $\tilde{\cdot}$, $\bar{\cdot}$ and $\hat{\cdot}$ over the signal denotes the data corrupted with frequency offset, unitary transformation of the data and estimated data, respectively. Bold face small letters are used for vectors and bold face capital alphabets are for matrix representation.

2 Related work

In this section, we summarise the existing work from conventional MIMO systems relevant to our research. The related work is divided into two subsections: (i) blind source separation and (ii) blind carrier and timing synchronisation.

2.1 Blind source separation

Blind separation of multiple sources with multiple sensors or antennas at the receiver has been extensively explored in the literature [13, 16–25]. These algorithms can be categorised into three different classes: (i) algorithms based on information theory (including the maximum likelihood approach) [16–18], (ii) algorithms based on cumulants (including correlation) [13, 19–22] and (iii) algorithms based on constant modulus constraints [23–25]. The algorithms based on information theory include the maximum likelihood algorithms and the infomax algorithms [16–18]. The output of the separation system is achieved through minimising the mutual information or maximisation the entropy of the output signals. These algorithms have many tunable parameters and achieving good-quality separation is highly dependent on the tuning of their parameters [26]. The algorithms based on constant modulus constraints depend on multistage signal separation and/or gradient descent optimisation. Depending on the initialisation of gradient descent algorithms, constant modulus algorithms sometimes fail to achieve global convergence resulting in poor-quality source separation. Thus, their performance depends on initial tunable parameters such as step sizes [24]. The main advantage of cumulant based algorithms is that they can work off-the-shelf (no parameter tuning is required). The algorithms based directly on cumulants include second-order statistic (SOS)-based algorithms [19, 20] and higher-order statistic (HOS)-based algorithms [13, 21, 22]. For these algorithms, the minimisation of cross-cumulants or the maximisation of autocumulants are usually used to achieve source separation. Among cumulant-based algorithms, the joint approximate diagonalisation of eigen-matrices (JADE) by Cardoso and Souloumiac [13] is the most renowned and computationally efficient algorithm [22, 27].

2.2 Blind carrier and timing synchronisation

Many well-known techniques are available in the literature for blind or non-data aided (NDA) estimation of a single carrier frequency offset [14, 28–31]. These methods can be classified into two main types: (i) algorithms that operate in feedback mode and employ automatic frequency control (AFC), which has the purpose of tracking the frequency offset in a closed-loop system [28, 29] and (ii) algorithms which operate in feed-forward mode and are based on open-loop frequency estimation [14, 30, 31]. Closed-loop schemes are more suitable for continuous mode transmission. However, in applications, where data are transmitted in short bursts or frames, or in applications where a fast reacquisition after a deep fade is required, the acquisition of an AFC loop may possibly last too long [32]. Therefore open-loop schemes are more appealing for frame-based transmission schemes because of their short estimation times [33]. In [14], a thorough analysis of the statistical properties of open-loop non-linear least square

© The Institution of Engineering and Technology 2011

(NLS) carrier synchronisers is provided and a blind carrier offset estimator with improved performance is proposed. It is important to note that this algorithm can work even in the presence of an unknown timing offset.

Blind or NDA estimation of a single unknown timing offset is also a well-established area of research [15, 34, 35]. The proposed solutions can be classified into two categories: (i) feedback algorithms which derive an estimate of the timing error and feed the corrective signal back to interpolator [15, 35] and (ii) feed-forward algorithms in which the timing offset estimate is derived from the received signal before it is corrected in the interpolator [15]. In frame-based transmission systems, where fast timing recovery is needed, feed-forward recovery schemes are more appealing because of faster acquisition time [15].

3 System model

We consider a (distributed-M) $\times$ N system where there are M distributed users, each with a single antenna, transmitting independent information to a common destination equipped with an array of N antenna elements as shown in Fig. 1. We consider frame-based transmission by each user. The number of co-channel users is assumed to be known to the destination. The transmitted baseband signal $s_m(t)$ for a user m is given by [33]

$$s_m(t) = \sum_{k=0}^{D-1} u_m(k)\, g_T(t - kT), \quad \text{for} \quad m = 1, \ldots, M \tag{1}$$

where the complex-valued symbols $u_m(k)$ denote the data symbols transmitted by the user m at the discrete time instant k, $g_T(t)$ is the transmitter pulse shaping filter for the digital communication system under consideration and is assumed the same for all users, T is the symbol period and D is the frame length for each user. Let the vector $\boldsymbol{u}_m$ be the source input vector containing D symbols for the user m and L_g be the approximate effective duration of the tail of $g_T(t)$ on one side.

The signal for each user is modulated by the carrier frequency $\omega + \omega_m$, as illustrated in Fig. 1, where ω_m is the analogue frequency offset between the user m and the receiver. All the demodulators are fed by the same oscillator with frequency ω, resulting in M frequency offsets in total. Ideally, ω_m should be zero for each user. However, in practice, the component inaccuracies in commercial-quality semiconductor radio frequency (RF) oscillators can amount to as much as a few parts per million. For a carrier frequency in GHz range, this can translate to a frequency offset of several hundred hertz and hence needs to be mitigated.

The demodulated signal for antenna i is given as

$$\tilde{y}_{i,\tau}(t) = \sum_{m=1}^{M} a_{m,i} \sum_{k=0}^{D-1} u_m(k)\, g_T(t - kT - \tau_m T)\, \mathrm{e}^{\mathrm{j}\tilde{\omega}_m t} + v_i(t) \tag{2}$$

where $\tilde{y}_{i,\tau}(t)$ is the baseband received signal at the antenna i for $i = 1, \ldots, N$, subscript 'τ' denotes the time delay between the transmitter and the receiver, '$\tilde{\ }$' over the signal denotes the frequency offset, $a_{m,i}$ is the component of spatial signature of the user m representing the gain or response of the antenna i to the user m, τ_m, normalised by the symbol duration T, is the fractional unknown timing offset ($|\tau_m| \leq 1/2$) for user m, $v_i(t) = n_i(t)\, \mathrm{e}^{-\mathrm{j}\tilde{\omega}t}$ is the complex noise at the antenna i with variance σ_v^2 where $n_i(t)$ is the white, zero-mean stationary, complex Gaussian process at the input of antenna i and '$*$' represents the convolution operator.

After pulse shaping at each receiver antenna, the signal is sampled with some timing offset since the receiver does not know the exact sampling point corresponding to maximum signal-to-noise ratio (SNR). The receiver filter output is then oversampled by a factor Q such that the oversampling period is $T_s = T/Q$. We assume that all the samplers at each receive antenna operate at the same time instant. Hence, (2) becomes

$$\tilde{y}_{i,\tau}(bT_s) = \sum_{m=1}^{M} a_{m,i} \sum_{k=0}^{D-1} u_m(k)\, g_T(bT_s - kT - \tau_m T) \times \mathrm{e}^{\mathrm{j}2\pi f_m b} + v_i(bT_s) \tag{3}$$

where b is the sampling index, $\omega_m t = \omega_m b T_s = 2\pi(F_m/F_s)b$, F_m is the frequency offset in Hz and $f_m = F_m/F_s$ is the digital frequency offset in cycles/sample for the user m.

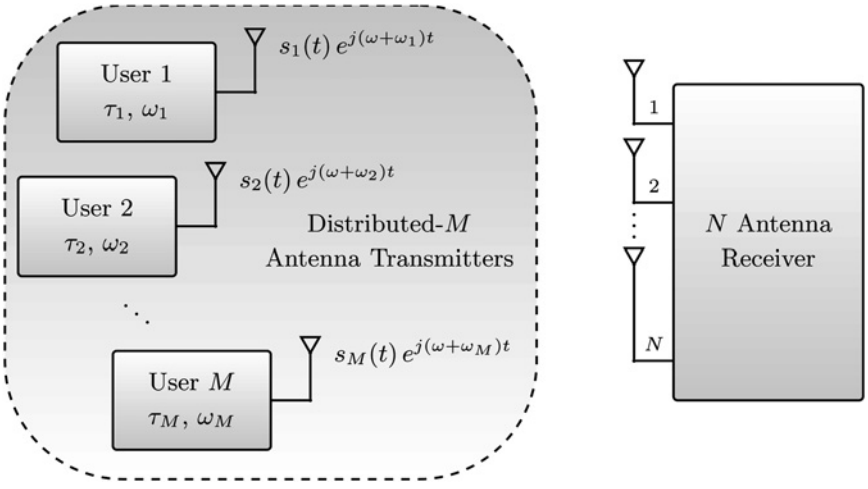

Fig. 1 *Distributed multiple users communicating with single receiver, in a (distributed-M) $\times$ N configuration*

© The Institution of Engineering and Technology 2011

doi: 10.1049/iet-com.2010.0528

The inner summation in (3) does not depend on i and so we can define this factor separately as

$$\tilde{s}_{m,\tau_m}(bT_s) = \sum_{k=0}^{D-1} u_m(k)\, g_T(bT_s - kT - \tau_m T)\, e^{j2\pi f_m b} \quad (4)$$

where $\tilde{s}_{m,\tau_m}$ is the oversampled pulse-modulated data for user m with timing and frequency offset τ_m and f_m, respectively. Thus, (3) can be written as

$$\tilde{y}_{i,\tau}(b) = \sum_{m=1}^{M} a_{m,i}\tilde{s}_{m,\tau_m}(b) + v_i(b) \quad (5)$$

where the index b corresponds to the samples at oversampling interval T_s.

Using (5), we can write the system model in compact matrix form as

$$\boldsymbol{Y} = \boldsymbol{A}\,\tilde{\boldsymbol{S}}_\tau + \boldsymbol{N} \quad (6)$$

where the matrices are defined as

$$\boldsymbol{Y} \triangleq [\tilde{\boldsymbol{y}}_{1,\tau}, \tilde{\boldsymbol{y}}_{2,\tau}, \ldots, \tilde{\boldsymbol{y}}_{N,\tau}]^T \quad (7)$$

$$\boldsymbol{A} \triangleq [\boldsymbol{a}_1, \boldsymbol{a}_2, \ldots, \boldsymbol{a}_M] \quad (8)$$

$$\tilde{\boldsymbol{S}}_\tau \triangleq [\tilde{\boldsymbol{s}}_{1,\tau_1}, \tilde{\boldsymbol{s}}_{2,\tau_2}, \ldots, \tilde{\boldsymbol{s}}_{M,\tau_M}]^T \quad (9)$$

$$\boldsymbol{N} \triangleq [\boldsymbol{v}_1, \boldsymbol{v}_2, \ldots, \boldsymbol{v}_N]^T \quad (10)$$

and the vectors are defined as

$$\tilde{\boldsymbol{y}}_{i,\tau} \triangleq [\tilde{y}_{i,\tau}(0), \tilde{y}_{i,\tau}(T_s), \ldots, \tilde{y}_{i,\tau}((R-1)T_s)] \quad (11)$$

$$\boldsymbol{a}_m \triangleq [a_{m,1}, a_{m,2}, \ldots, a_{m,N}]^T \quad (12)$$

$$\tilde{\boldsymbol{s}}_{m,\tau_m} \triangleq [\tilde{s}_{m,\tau_m}(0), \tilde{s}_{m,\tau_m}(T_s), \ldots, \tilde{s}_{m,\tau_m}((R-1)T_s)] \quad (13)$$

$$\boldsymbol{v}_i \triangleq [v_i(0), v_i(T_s), \ldots, v_i((R-1)T_s)]^T \quad (14)$$

where superscript $(\cdot)^T$ denotes the transpose of a vector, $R \triangleq (D + 2L_g)Q$, $\tilde{\boldsymbol{y}}_{i,\tau}$ is the demodulated output vector of antenna i, $\tilde{\boldsymbol{s}}_{m,\tau_m}$ is the signal vector for user m corrupted by timing and carrier offsets, $\boldsymbol{a}_m$ is the channel vector for user m and $\boldsymbol{v}_i$ is the filtered noise vector at antenna i.

The 'joint blind timing and carrier synchronisation problem' in a (distributed-M) $\times$ N system is to estimate the M carrier offsets and M timing offsets and to recover the transmitted symbols for each user given only the measured signal at each antenna, with no initial training.

4 Proposed blind receiver architecture

The receiver can be divided into three separate blocks: (i) blind source separation, (ii) carrier offset recovery and (iii) timing recovery, as shown in Fig. 2. The blind source separation block performs the channel estimation to decouple the source mixing and provides an estimate of each user's data corrupted by timing and frequency offsets $\hat{\tilde{\boldsymbol{s}}}_{m,\tau_m}$. Note that $\hat{\tilde{\boldsymbol{s}}}_{m,\tau_m} \triangleq [\hat{\tilde{s}}_{m,\tau_m}(0), \hat{\tilde{s}}_{m,\tau_m}(T_s), \ldots, \hat{\tilde{s}}_{m,\tau_m}((R-1)T_s)]$ is an estimate of $\tilde{\boldsymbol{s}}_{m,\tau_m}$ which is defined in (13). The separated user signals are passed to the frequency offset recovery block which estimates the carrier offset and outputs each user's signal, $\hat{\boldsymbol{s}}_{m,\tau_m}$, corrupted only by the timing offset. The timing offset recovery block estimates the timing offset, $\hat{\tau}_m$, for user m, and the signal at the input of the timing estimation block is match filtered with an impulse response $g_R(t + \hat{\tau}_m)$ matched to the transmit filter $g_T(t)$. The output of matched filter block yields the estimate of the user m data vector $\hat{\boldsymbol{u}}_m \triangleq [\hat{u}_m(0), \hat{u}_m(T_s), \ldots, \hat{u}_m((R-1)T_s)]$, as shown in Fig. 2. The detailed working of these blocks is discussed in the subsections below.

4.1 Blind source separation

The blind source separation technique we choose is based on the JADE algorithm [13] and is illustrated in Fig. 3. The JADE algorithm requires some form of diversity in the received mixture of signals for its proper operation [12, 13]. The diversity order should be greater than or equal to the number of independent user signals that need to be separated. In this work, we have used N antennas at the destination ($N \geq M$ where M is the number of independent users) to provide the required diversity in the received mixture of signals for JADE algorithm.

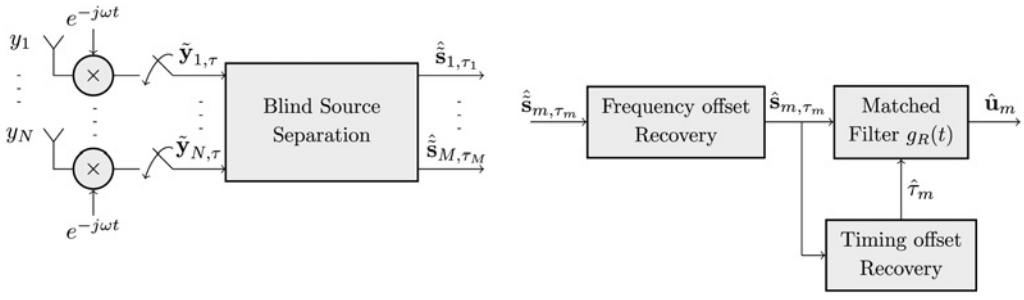

Fig. 2 *Proposed receiver block diagram for joint blind source separation and timing and carrier synchronisation*

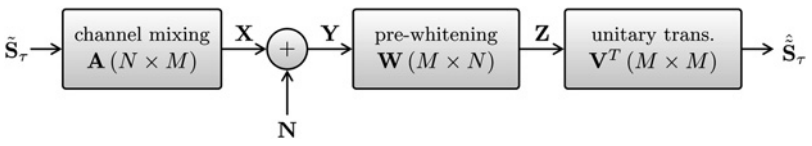

Fig. 3 *Block diagram of blind source separation based on JADE algorithm*

© The Institution of Engineering and Technology 2011

The JADE algorithm assumes that the input signals are statistically independent and have non-gaussian distribution [36]. According to the Central Limit Theorem, the channel mixing of the independent (non-gaussian) sources $\boldsymbol{u}_m$ results in signals at each antenna, $\tilde{\boldsymbol{y}}_{i,\tau}$, having a distribution which is close to Gaussian [36]. Thus, the blind source separation objective is to apply some linear transformation to $\boldsymbol{Y}$ to maximise the non-gaussianity of the output $\hat{\tilde{\boldsymbol{S}}}_\tau$. Achieving this objective requires three main steps:

Step 1: The first step is pre-whitening which makes the observed components $\tilde{\boldsymbol{y}}_{i,\tau}$ uncorrelated. The utility of whitening resides in the fact that it transforms the mixing matrix $\boldsymbol{A}$ into a unitary matrix, which eases the further estimation procedure. For whitening, we use eigen-value decomposition (EVD) of the covariance matrix of received signal $\boldsymbol{R}_{\boldsymbol{Y}} = E\{\boldsymbol{Y}\boldsymbol{Y}^{\mathrm{H}}\} = \boldsymbol{E}\boldsymbol{\Lambda}\boldsymbol{E}^{\mathrm{H}}$, where $\boldsymbol{E}$ is the unitary matrix of eigenvectors of $\boldsymbol{R}_{\boldsymbol{Y}}$ and $\boldsymbol{\Lambda}$ is the diagonal matrix of its eigenvalues. The whitening matrix $\boldsymbol{W}$ is computed as

$$\boldsymbol{W} = \boldsymbol{R}_{\boldsymbol{Y}}^{-1/2} = \boldsymbol{E}\boldsymbol{\Lambda}^{-1/2}\boldsymbol{E}^{\mathrm{H}} \tag{15}$$

Applying pre-whitening the whitened matrix $\boldsymbol{Z}$, as shown in the Fig. 3, is given as

$$\boldsymbol{Z} = \boldsymbol{W}\boldsymbol{Y} = \tilde{\boldsymbol{A}}\,\tilde{\boldsymbol{S}}_\tau + \boldsymbol{W}\boldsymbol{N} \tag{16}$$

where $\tilde{\boldsymbol{A}} = \boldsymbol{W}\boldsymbol{A}$ is a new mixing matrix. The whitened matrix $\boldsymbol{Z}$ accommodates the resulting uncorrelated components $\boldsymbol{z}_m$, where $\boldsymbol{Z} \triangleq [\boldsymbol{z}_1, \boldsymbol{z}_2, \ldots, \boldsymbol{z}_M]^{\mathrm{T}}$ and $\boldsymbol{z}_m \triangleq [z_m(0), z_m(T_{\mathrm{s}}), \ldots, z_m((R-1)T_{\mathrm{s}})]$. Note that the signal part of $\boldsymbol{Z}$ is a unitary mixture of input signal components $\tilde{\boldsymbol{s}}_{m,\tau_m}$.

Step 2: The next step is to determine the unitary transformation matrix $\boldsymbol{V}$. This is determined according to the JADE criterion. To determine $\boldsymbol{V}$ using the whitened received signal matrix $\boldsymbol{Z}$, we proceed as follows. Let $\mathcal{Q}_{k,l} = \mathrm{Cum}(\boldsymbol{z}_i, \boldsymbol{z}_j, \boldsymbol{z}_k, \boldsymbol{z}_l)$ for $1 \le i, j \le M$ represent the (k, l)th cumulant matrix such that $1 \le k, l \le M$ and Cum$(\cdot)$ denote the cumulant operation [22]. Note that in this case there will be M^2 cumulant matrices in total. We stack all the cumulant matrices $\mathcal{Q}_{k,l}$ into a single $M^2 \times M^2$ matrix $\mathcal{Q}_{a,b}$, where $a = i + (j-1)M$ and $b = l + (k-1)M$. Taking EVD of $\mathcal{Q}_{a,b}$, we get $\mathcal{Q}_{a,b}\mathcal{M} = \mathcal{M}\mathcal{V}$, where $\mathcal{M}$ accommodates the eigenvectors of $\mathcal{Q}_{a,b}$ and $\mathcal{V}$ is the diagonal matrix containing its eigenvalues $(\lambda_1, \lambda_2, \ldots, \lambda_{M^2})$. Then we unstack each column of $\mathcal{M}$ into an $M \times M$ matrix by inserting the entries columnwise, resulting in M^2 eigenmatrices $\{\mathcal{E}_1, \mathcal{E}_2, \ldots, \mathcal{E}_{M^2}\}$. Let $\mathcal{N}^e = \{\lambda_d \mathcal{E}_d \mid 1 \le d \le M\}$ be the eigen-set of M most significant eigen-pairs of the unstacked matrices, corresponding to M most significant eigenvalues. We perform joint diagonalisation of this set $\mathcal{N}^e$ under the unitary constraint $\boldsymbol{V}$, resulting in JADE maximisation criteria $C(\boldsymbol{V}, \mathcal{N}^e) = \sum_{d=1}^{M} |\mathrm{diag}(\boldsymbol{V}^{\mathrm{H}}\lambda_d\mathcal{E}_d\boldsymbol{V})|^2$. Finally, $\boldsymbol{V}$ is obtained by performing Joint diagonalisation of $M \times M$ matrices $\mathcal{R}_d = \lambda_d\mathcal{E}_d$, $d = 1, \ldots, M$ using the above maximisation criteria, as detailed in [37]. Note that with correct operation, the above procedure will converge the output towards $\boldsymbol{V} = \tilde{\boldsymbol{A}}$.

Step 3: The third and final step is to use $\boldsymbol{V}$ to separate the sources. The output of the blind source separation block is given by

$$\begin{aligned}\hat{\tilde{\boldsymbol{S}}}_\tau &= \boldsymbol{V}^{\mathrm{H}}\boldsymbol{Z} \\ &= \boldsymbol{V}^{\mathrm{H}}\tilde{\boldsymbol{A}}\tilde{\boldsymbol{S}}_\tau + \boldsymbol{V}^{\mathrm{H}}\boldsymbol{W}\boldsymbol{N}\end{aligned} \tag{17}$$

It can be seen that if $\boldsymbol{V} = \tilde{\boldsymbol{A}}$, then $\boldsymbol{V}^H\tilde{\boldsymbol{A}} = \boldsymbol{I}_M$ and the components of $\hat{\tilde{\boldsymbol{S}}}_\tau$ will be free from channel mixing, though with embedded timing and frequency offsets and noise corruption. Note that $\boldsymbol{A} = \boldsymbol{W}^{-1}\tilde{\boldsymbol{A}}$ is evaluated upto a permutation and scaling of its columns. This is a well-known fundamental limitation common to all blind schemes [12, 13, 38]. In this work, we have resolved this ambiguity by assuming a known single symbol transmission for each source, occupying M time slots in total [38].

4.2 Frequency offset recovery

After blind source separation, each of the separated signals $\hat{\tilde{\boldsymbol{s}}}_{m,\tau_m}$ can be written as

$$\hat{\tilde{s}}_{m,\tau_m}(bT_{\mathrm{s}}) = \sum_{k=0}^{D-1} u_m(k) g_T(bT_{\mathrm{s}} - kT - \tau_m T)\mathrm{e}^{\mathrm{j}2\pi f_m b} + \check{v}_{m,W}(bT_{\mathrm{s}}) \tag{18}$$

where $\hat{\tilde{s}}_{m,\tau_m}(bT_{\mathrm{s}})$ is an element of $\hat{\tilde{\boldsymbol{s}}}_{m,\tau_m}$, '$\hat{\cdot}$' over the signal denotes the estimated data, $\check{v}_{m,W}(b)$ is an element of sequence m of $\boldsymbol{V}^{\mathrm{H}}\boldsymbol{W}\boldsymbol{N}$ and represents the noise term after source separation.

The frequency offset estimation relies on the cyclostationary statistics of the oversampled received signal [14]. The algorithm can estimate the frequency offset up to one-eighth times the symbol rate $1/T$, that is, $|F_m T| \le 1/8$, where $F_m = \omega_m/2\pi$, which is very reasonable handling capability [39]. The frequency offset estimator for the user m is given as

$$\hat{f}_m = \frac{1}{Q}\arg \max_{|\dot{\alpha}|<1/(2Q)} J_R(\dot{\alpha}) \tag{19}$$

where $R = (D + 2L_g)Q$ is the length of received vector $\hat{\tilde{\boldsymbol{s}}}_{m,\tau_m}$ and $\dot{\alpha}$ is the trial value of the cyclic frequency in the objective function $J_R(\dot{\alpha})$, which is given by

$$J_R(\dot{\alpha}) = \sum_{j=0}^{Q-1} |\hat{\tilde{C}}_4(\dot{\alpha} + j/Q; \mathbf{0})|^2 \tag{20}$$

where $\mathbf{0} = [0\ 0\ 0]$ and $\hat{\tilde{C}}_4(\dot{\alpha} + j/Q; \mathbf{0})$ is the asymptotic sample estimator of the true cyclic correlation of fourth-order time-varying correlation function $\tilde{c}_4(b; \mathbf{0})$ of the received sequence $\hat{\tilde{s}}_{m,\tau_m}(b)$, given as

$$\hat{\tilde{C}}_4(\dot{\alpha} + j/Q; \mathbf{0}) = \frac{1}{R}\sum_{b=0}^{R-1} \hat{\tilde{s}}^4_{m,\tau_m}(b)\,\mathrm{e}^{-\mathrm{j}2\pi(\dot{\alpha}+j/Q)b} \tag{21}$$

where $\tilde{c}_4(b; \mathbf{0}) = E\{\hat{\tilde{s}}^4_{m,\tau_m}(b)\}$. Substituting (21) into (20), we obtain the estimator as

$$J_R(\dot{\alpha}) = \sum_{j=0}^{Q-1} \left| \frac{1}{R}\sum_{b=0}^{R-1} \hat{\tilde{s}}^4_{m,\tau_m}(b)\,\mathrm{e}^{-\mathrm{j}2\pi(\dot{\alpha}+j/Q)b} \right|^2$$

Remark: Equation (20) implies that $\dot{\alpha}$ is the cyclic frequency for the conjugate cyclic correlation and summation over $j = 0, 1, \ldots, Q-1$ is used to extract the frequency offset by exploiting jointly the location information of all Q spectral lines.

© The Institution of Engineering and Technology 2011

doi: 10.1049/iet-com.2010.0528

4.3 Timing offset recovery

After frequency offset estimation, we are left with the signal $\hat{\boldsymbol{s}}_{m,\tau_m}$ for the user m, which can be written as

$$\hat{s}_{m,\tau_m}(bT_s) = \sum_{k=0}^{D-1} u_m(k)\, g_T(bT_s - kT - \tau_m T) + \check{v}_{m,W}(bT_s)\, e^{-j2\pi f_m b} \quad (22)$$

The prior requirement on the sampling rate of the signal $\hat{s}_{m,\tau_m}(b)$ must be such that the spectral component at $1/T$ can still be represented, that is, $Q/T > 2/T$. The input signal $\hat{s}_{m,\tau_m}(b)$ is absolute squared to obtain $p(b) = |\hat{s}_{m,\tau_m}(b)|^2$ and resultant signal contains a spectral component at $1/T$. This spectral component is determined for every section of length LT (i.e. from LQ samples) by computing the complex fourier coefficient at the symbol rate

$$P_r = \sum_{\ell=rQL}^{(r+1)LQ-1} p(\ell)\, e^{-j2\pi\ell/Q} \quad (23)$$

where r corresponds to different sections of length QL of the squared input signal $p(b)$, for $r = 1, \ldots, \lfloor R/LQ \rfloor$. The normalised timing offset τ_m is then computed by using the argument of expected value of P_r over all the sections [15]

$$\hat{\tau}_m = E_r\left\{-\frac{1}{2\pi}\arg(P_r)\right\} \quad (24)$$

Finally, the estimate of each user signal $\hat{\boldsymbol{u}}_m$ can be found by matching the filtering signal $\hat{s}_{m,\tau_m}(b)$ with the delay $\hat{\tau}_m$ that is opposite to the introduced offset.

5 Performance analysis

To benchmark the performance of our estimators, we use Modified Cramer-Rao Bound (MCRB) for carrier and timing offset estimation respectively. MCRB for carrier offset estimation is given as [33]

$$\mathrm{MCRB}(f) = \frac{3\sigma_v^2}{2\pi^2 D^3 Q^2} \quad (25)$$

where σ_v^2 is the variance of complex filtered noise, D is the frame length and Q is the oversampling factor. Similarly, MCRB for timing offset estimation is given as [33]

$$\mathrm{MCRB}(\tau) = \frac{\sigma_v^2}{8\pi^2 \eta D} \quad (26)$$

where $\eta = (1/12) + \beta^2((1/4) - (2/\pi^2))$ and β is the roll-off factor of root-raised cosine pulse.

It must be noted that the above bounds have been presented in the literature for a single transmitter and single receiver scenario. In our case, since timing and frequency offsets for each user are estimated separately after achieving source separation, we argue that these bounds can provide a loose benchmark owing to the self-noise of blind source separation block. Moreover, we have used the same benchmark for different number of receive antennas, N, considering the fact that even if the data are recovered from the antenna with high received SNR, the estimator performance will still be bounded by the same MCRB. This is because in our proposed receiver, multiple antennas are only used to achieve blind source separation. The derivation of tighter bounds is an open problem.

6 Simulation results

In this section, simulation results are presented to validate the robustness of the proposed blind receiver algorithm. The scenario considered includes $M = 4$ distributed users, communicating with an N antenna receiver. Each user employs quadrature phase shift keying (QPSK) modulation and transmits data in frames of length D. The root-raised cosine filters are used for transmitter pulse shaping and receiver-matched filtering, with roll-off factor $\beta = 0.25$ and filter tap delay length $L_g = 5$. The oversampling factor used is $Q = 4$ in order to meet the requirement mentioned in Section 4.3. The parameter L in (23) is set to 16. The unknown timing offsets τ_m for M users are assumed to be uniformly distributed as ($|\tau_m| \leq 1/2$). The unknown digital frequency offsets f_m for M users are assumed to be uniformly distributed as $|f_m| \leq 1/32$. This follows from the constraint on the frequency offset, $|F_m T| \leq 1/8$, as mentioned in Section 4.2. We use 500 steps for $\dot{\alpha}$ in the frequency offset estimation range in (19).

The system performance is analysed as a function of the number of receive antennas N and frame lengths D, respectively, for two different channel models:

- i.i.d. channel model in which the complex channel coefficients are i.i.d. from frame to frame but remain constant for a particular frame.
- Rayleigh fading model with single tap in which the complex channel coefficients are time varying with certain correlation factor within a frame because of Doppler frequency f_D.

The figures of merit used are the BER, the mean square error (MSE) of the frequency offsets and the MSE of the timing offsets, respectively. These are calculated as follows:

1. The BER is calculated as the average of BERs from all users, that is, $\mathrm{BER} = (1/M)\sum_{m=1}^{M} \mathrm{BER}(m)$, where $\mathrm{BER}(m)$ is the BER for the user m.
2. The MSE of frequency offsets is calculated using the formulation, $(1/M)\sum_{m=1}^{M}(\hat{f}_m - f_m)^2$, in which the MSE of all the users is averaged out.
3. The MSE of timing offsets is calculated using the formulation, $(1/M)\sum_{m=1}^{M}(\hat{\tau}_m - \tau_m)^2$, in which the MSE of all the users is averaged out.

All the simulation results are averaged over $((5 \times 10^6)/(D \times Q \times M))$ Monte Carlo simulation runs for each value of SNR.

6.1 i.i.d channel model

6.1.1 BER performance: Fig. 4 shows the BER of the proposed blind system as a function of SNR (dB). Fig. 4*a* shows the BER with $M = 4$ distributed users, frame length $D = 400$ and $N = 4, 5, 6$ antenna receiver, respectively. It can be seen that increasing the number of receiver antennas improves the BER because of improved blind source separation. In addition, it can be seen that there is no observable error floor in the wide range of SNR values shown in the figure. The results show that increasing the

© The Institution of Engineering and Technology 2011

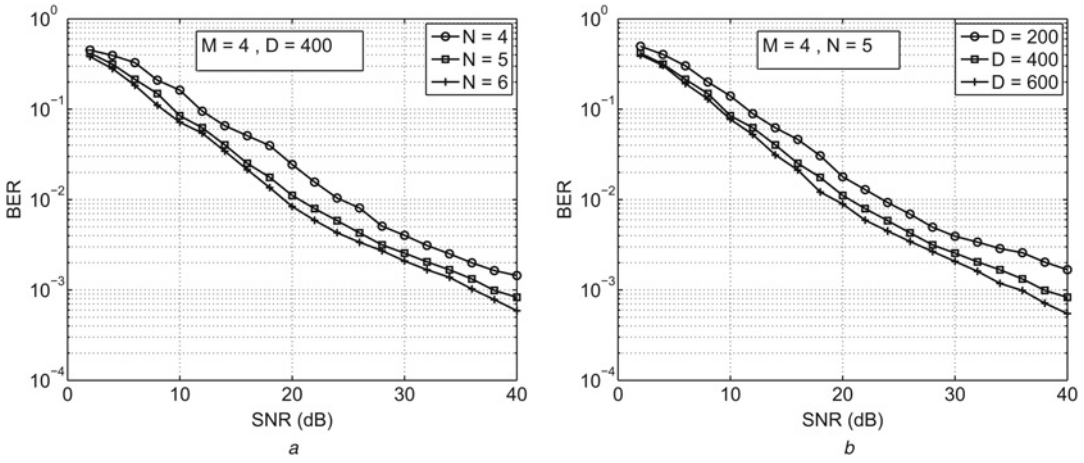

Fig. 4 *BER of the proposed blind system as a function of SNR (dB) for $M = 4$ distributed users, i.i.d. channel model and assuming*

a Frame length $D = 400$ symbols and $N = 4, 5, 6$ antenna receiver
b $N = 5$ antenna receiver and frame length $D = 200, 400, 600$ symbols, respectively

number of antennas at the receiver from 4 to 5 considerably improves the BER performance, for example, at 15 dB the BER improvement is about 52%. However, increasing the number of receiver antennas from 5 to 6 results in diminishing returns. We have observed this trend for different number of distributed users. This suggests that for a (distributed M) $\times$ N system, $N = M + 1$ antenna receiver yields close to best performance, while increasing N further results in diminishing returns.

Fig. 4*b* shows the BER with $M = 4$ distributed users, $N = 5$ antenna receiver and frame lengths $D = 200, 400, 600$, respectively. It can be seen that increasing the frame length improves the BER because of better estimation of timing and frequency offsets and improvement in blind source separation performance. In addition, there is considerable performance improvement in going from a frame length of 200 to as few as 400 symbols but only very minor improvement in increasing the frame length from 400 to 600 symbols.

6.1.2 Frequency offset estimation performance:

Fig. 5 shows the MSE of the frequency offset estimation as a function of SNR (dB). The MCRB from (25) is plotted as a loose reference. Fig. 5*a* shows the MSE of frequency offset estimation with $M = 4$ distributed users, frame length $D = 400$ and $N = 4, 5, 6$ antenna receiver, respectively. It can be seen that the MSE decreases (as expected) with increasing values of SNR and also by increasing the number of receiver antennas which leads to better source separation prior to carrier offset recovery. The performance is relatively poor for $N = 4$ receiver antennas but improves considerably with $N = 5$ receiver antennas. Similar to the previous case, there are diminishing returns in going from $N = 5$ to $N = 6$ receiver antennas. Fig. 5*b* shows the MSE of frequency offset estimation with $M = 4$ distributed users, $N = 5$ antenna receiver and frame lengths $D = 200, 400, 600$, respectively. This figure illustrates the effect of frame length on the frequency offset estimation performance. It can be seen that the performance is relatively poor for a frame length of $D = 200$ symbols, which is too small, but improves considerably as the frame length is increased.

Note that the MCRB bound is loose in both graphs of Fig. 5 because of the self-noise of blind source separation algorithm and also because the MCRB calculated for the ease of calculation is less than the actual CRB [33]. We can see from Fig. 5 that after a certain SNR the MSE drops quickly

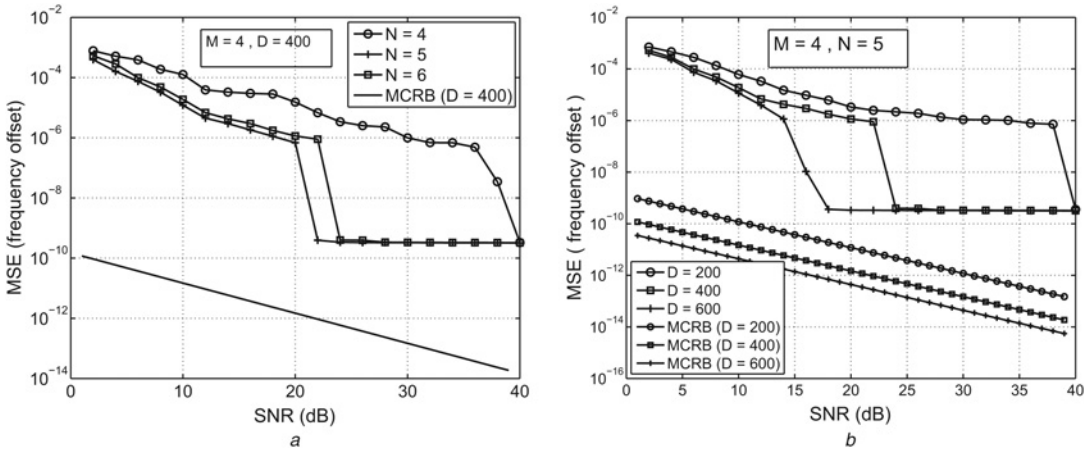

Fig. 5 *Mean square error of frequency offset estimation as a function of SNR (dB) for $M = 4$ distributed users, i.i.d. channel model and assuming*

a Frame length $D = 400$ symbols and $N = 4, 5, 6$ antenna receiver
b $N = 5$ antenna receiver and frame length $D = 200, 400, 600$ symbols, respectively

© The Institution of Engineering and Technology 2011

doi: 10.1049/iet-com.2010.0528

and converges to the minimum possible value for a given step size in the frequency offset estimation algorithm. Note that this effect is commonly observed in the MSE performance of frequency offset estimation algorithms [14, 40–42]. We can also see from Fig. 5 that at sufficiently high SNR all the curves reach the same error floor. This error floor at higher values of SNR in the simulated curves for both graphs is because of maximising the metric over finite set of values of $\dot{\alpha}$ in (20).

6.1.3 Timing offset estimation performance: Fig. 6 shows the MSE of the timing offset estimation as a function of SNR (dB) with $M = 4$ distributed users and Fig. 6*a* frame length $D = 400$ and $N = 4, 5, 6$ antenna receiver and Fig. 6*b* $N = 5$ antenna receiver and frame lengths $D = 200, 400, 600$, respectively. The MCRB from (26) is plotted as a reference. It can be seen from the two figures that the bound is very loose because of the self-noise of both the blind source separation and frequency offset estimation blocks and also because the MCRB calculated for the ease of calculation is lesser than the actual CRB [33]. In addition, the results show that timing offset is the least sensitive parameter and the performance is not much improved by increasing either the number of antennas or the frame length. This trend is because of the fact that timing offset is estimated last in our proposed receiver.

6.2 Rayleigh fading channel model

In this section, we consider the case of a (distributed-$M = 4$) $\times$ $N = 5$ system and evaluate the performance by varying the frame length D and the doppler frequency f_D, respectively. The carrier frequency is chosen as $f_c = 2$ GHz, which is a typical value. The relative velocity between the transceivers is set to $v = 140$ km/h, which corresponds to a very high Doppler frequency of $f_D = 259$ Hz. The symbol time is set to $T = 0.1$ μs to provide appropriate correlation ($J_o(2\pi f_D DT) > 0.99$) [43] of the channel coefficients within a frame period.

Fig. 7*a* shows MSE performance of frequency offset estimation, Fig. 7*b* MSE performance of timing offset estimation and Fig. 7*c* BER performance for the above scenario, respectively. It can be seen that the performance improves as the number of symbols in a frame increases from $D = 200$ to 400 because of better estimation of frequency and timing offsets. However, as the frame length increases from $D = 400$ to 600 symbols, the performance degrades for all the three metrics. This degradation is

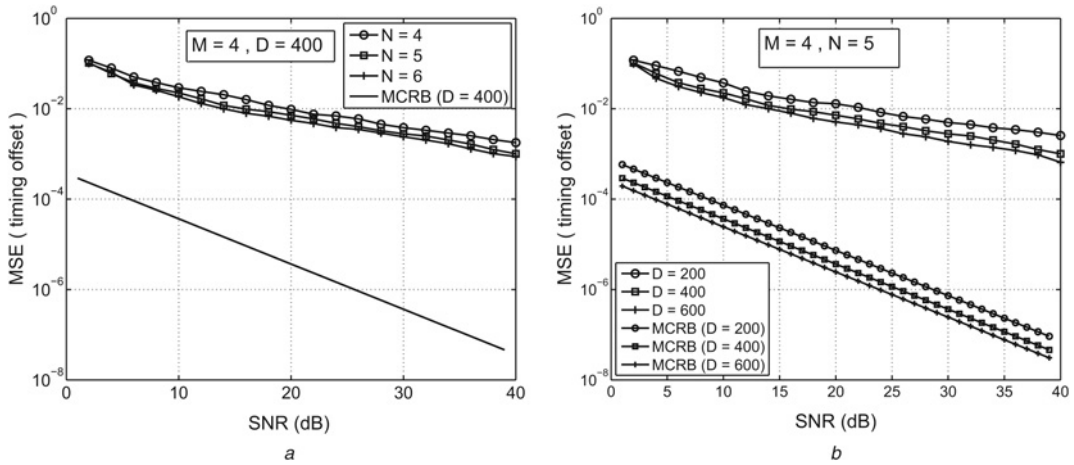

Fig. 6 *Mean square error of timing offset estimation as a function of SNR (dB) for $M = 4$ distributed users, i.i.d. channel model and assuming*

a Frame length $D = 400$ symbols and $N = 4, 5, 6$ antenna receiver
b $N = 5$ antenna receiver and frame length $D = 200, 400, 600$ symbols, respectively

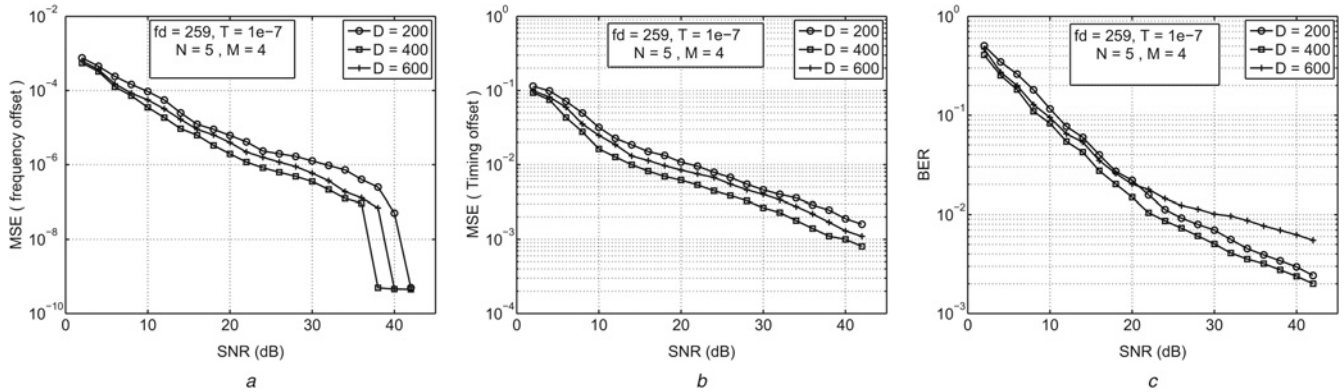

Fig. 7 *System performance for (distributed $M = 4$) $\times$ ($N = 5$) system as a function of SNR (dB) for Doppler frequency (f_D) = 259 Hz, symbol time $T = 0.1$ μs and frame length $D = 200, 400, 600$ symbols, respectively*

a MSE of frequency offsets
b MSE of timing offsets
c BER performance

© The Institution of Engineering and Technology 2011

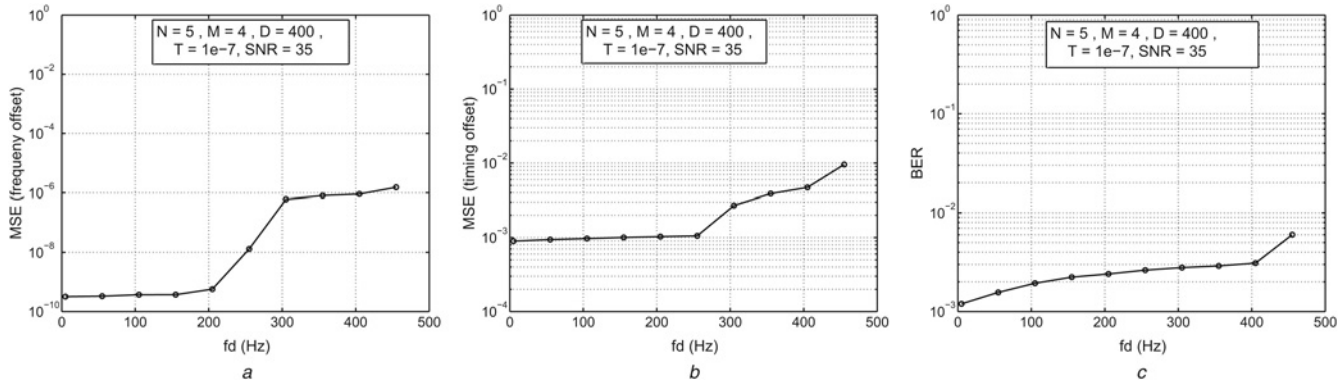

Fig. 8 *System performance for (distributed $M = 4$) × ($N = 5$) system as a function of Doppler frequency for symbol time $T = 0.1$ μs, frame length $D = 400$ symbols and SNR = 35 dB*

a MSE of frequency offsets
b MSE of timing offsets
c BER performance

because of the effect of decorrelation of channel coefficients that becomes dominant with larger frame size. Note that this trend is different and was not present in the case of i.i.d. channel model as the channel coefficients were constant within a frame.

Fig. 8*a* shows MSE performance of frequency offsets estimation, Fig. 8*b* MSE performance of timing offset estimation and Fig. 8*c* BER performance, respectively, for the above scenario as function of Doppler frequency f_D at SNR = 35 dB. The results show that the performance degrades as we increase the doppler frequency because of increase in time selectivity and decorrelation of the channel coefficients. However the degradation is very small for Doppler frequency $f_D < 300$ Hz, which shows the robustness of the proposed blind receiver performance. In addition, the receiver demonstrates reasonable uncoded BER performance even with the worst case doppler values, for example, a BER of 1×10^{-3} at a Doppler frequency of $f_D = 250$ Hz. This means that the system is capable of successfully handling a high data rate of 10 Msymbols/s provided the delay spread is less than ten times the symbol duration that is, less than 0.01 μs.

7 Conclusions

This paper has presented a receiver architecture for blind timing and carrier synchronisation in a distributed MIMO communication system. The proposed receiver is based on JADE algorithm for blind source separation and enables decoupling of the timing and carrier offsets from user to user. The proposed approach provides a robust, low-complexity alternative to the problem of joint estimation of multiple timing and frequency offsets. The simulation results confirm the excellent and robust performance of the proposed receiver under a wide range of parameter values. It has been shown that the for a (distributed-M) × N system, $N = M + 1$ antenna receiver yields close to best performance. In addition, the proposed receiver yields satisfactory results even with worst case Doppler of $f_D = 200-300$ Hz and frame size as small as 400 symbols.

8 References

1 Meitzner, J., Schober, R., Lampe, L., Gerstacker, W.H., Hoeher, P.A.: 'Multiple antenna techniques for wireless communications – a comprehensive literature survery', *IEEE Commun. Surv. Tuts*, 2009, **11**, (2), pp. 87–105

2 Gesbert, D., Shafi, M., Shiu, D.S., Smith, P.J., Naguib, A.: 'From theory to practice: an overview of MIMO space-time coded wireless systems', *IEEE J. Sel. Areas Commun.*, 2003, **21**, pp. 281–302

3 Sendonaris, A., Erkip, E., Aazhang, B.: 'User cooperation diversity, part I and II', *IEEE Trans. Commun.*, 2003, **51**, pp. 1927–1948

4 Hong, Y.W., Huang, W.J., Chiu, F.H., Kuo, C.C.J.: 'Cooperative communications in resource-constrained wireless networks', *IEEE Signal Process. Mag.*, 2007, **24**, (3), pp. 47–57

5 Ibrahim, A.S., Liu, R.: 'Mitigating channel estimation error with timing synchronization tradeoff in cooperative communications', *IEEE Trans. Signal Process.*, 2010, **58**, pp. 337–348

6 Palat, R.C., Annamalai, A., Reed, J.H.: 'Accurate bit-error-rate analysis of bandlimited cooperative OSTBC networks under timing synchronization errors', *IEEE Trans. Veh. Technol.*, 2009, **58**, (5), pp. 2191–2200

7 Parker, P.A., Mitran, P., Bliss, D.W., Tarokh, V.: 'On bounds and algorithms for frequency synchronization for collaborative communication systems', *IEEE Trans. Signal Process.*, 2008, **56**, (8), pp. 3742–3752

8 Rajawat, K., Chaturvedi, A.K.: 'Non data aided symbol timing estimation in MIMO systems'. Proc. ICC, 2007, pp. 5455–5461

9 Shahbazpanahi, S., Gershman, A.B., Giannakis, G.B.: 'Joint blind channel and carrier frequency offset estimation in orthogonally space time block coded MIMO systems'. IEEE Workshop on Signal Processing Advances in Wireless Communication, 2005, pp. 363–367

10 Oh, M., Ma, X., Giannakis, G., Park, D.: 'Cooperative synchronization and channel estimation in wireless sensor networks', *J. Commun. Netw.*, 2005, **7**, (3), pp. 284–293

11 Li, X., Wu, Y.C., Serpedin, E.: 'Timing synchronization in decode-and-forward cooperative communication systems', *IEEE Trans. Signal Process.*, 2009, **57**, (4), pp. 1444–1455

12 Petropulu, A.P., Olivieri, M., Yu, Y., Dong, L., Lackpour, A.: 'Pulse-shaping for blind multi-user separation in distributed MISO configurations'. Proc. IEEE ICASSP, 2008, pp. 2741–2744

13 Cardoso, J.F., Souloumiac, A.: 'Blind beamforming for non-Gaussian signals', *Proc. IEEE Radar Signal Process.*, 1993, **140**, pp. 362–370

14 Wang, Y., Shi, K., Serpedin, E.: 'Non data-aided feedforward carrier frequency offset estimators for QAM constellations: a nonlinear least-squares approach', *EURASIP J. Appl. Signal Process.*, 2004, **13**, pp. 1993–2001

15 Oerder, M., Meyr, H.: 'Digital filter and square timing recovery', *IEEE Trans. Commun.*, 1988, **36**, (5), pp. 605–612

16 Cardoso, J.F.: 'Infomax and maximum likelihood for blind source separation', *IEEE Signal Process. Lett.*, 1997, **4**, pp. 112–114

17 Vlassis, N., Motomura, Y.: 'Efficient source adaptivity in independent component analysis', *IEEE Trans. Neural Netw.*, 2001, **12**, (3), pp. 559–566

18 Bell, A.J., Sejnowski, T.J.: 'An information-maximization approach to blind separation and blind convolution', *Neural Comput.*, 1995, **7**, pp. 1129–1159

19 Chang, C., Ding, Z.: 'A matrix-pencil approach to blind separation of colored nonstationary signals', *IEEE Trans. Signal Process.*, 2000, **48**, (3), pp. 900–907

20 Yin, F., Mei, T., Wang, J.: 'Blind source separation based on decorrelation and nonstationarity', *IEEE Trans. Circuits Syst.*, 2007, **54**, (5), pp. 1150–1158

© The Institution of Engineering and Technology 2011

doi: 10.1049/iet-com.2010.0528

21 Papadias, C.B.: 'Globally convergent blind source separation based on a multiuser kurtosis maximization criterion', *IEEE Signal Process. Lett.*, 2000, **48**, (12), pp. 3508–3519
22 Mei, T., Yin, F., Wang, J.: 'Blind source separation based on cumulants with time and frequency non-properites', *IEEE Trans. Audio Speech Lang. Process.*, 2009, **17**, (6), pp. 1099–1108
23 Papadias, C.B., Paulraj, A.J.: 'A constant modulus algorithm for multiuser signal separation in presence of delay spread using antenna arrays', *IEEE Signal Process. Lett.*, 1997, **4**, pp. 178–181
24 Van Der Veen, A.J., Paulraj, A.: 'An analytical constant modulus algorithm', *IEEE Trans. Signal Process.*, 1996, **44**, (5), pp. 1136–1155
25 Yao, Y., Giannakis, G.B.: 'On regularity and identifiability of blind source separation under constant-modulus constraints', *IEEE Trans. Signal Process.*, 2005, **4**, (4), pp. 1272–1281
26 Li, Y., Powers, D., Peach, J.: 'Comparison of blind source separation algorithms'. Proc. WSES, Advances in Neural Networks and Applications, 2000, pp. 18–21
27 Liu, X., Kountouriotis, J., Petropulu, A.P., Dandekar, K.R.: 'ALOHA with collision resolution (ALOHA-CR): theory and software defined radio implementation', *IEEE Trans. Signal Process.*, 2010, **58**, pp. 4396–4410
28 Natali, F.D.: 'AFC tracking algorithms', *IEEE Trans. Commun.*, 1984, **32**, pp. 935–947
29 Andrea, A.N., Mengal, U.: 'Performance of a quradricorrelator driven by modulated signals', *IEEE Trans. Commun.*, 1990, **38**, (11), pp. 1952–1957
30 Ghogho, M., Swami, A., Durrani, T.: 'On blind carrier recovery in tme-selective fading channels'. Proc. 33rd Conf. on Signals, Systems and Computers, 1999, vol. 1, pp. 243–247
31 Gini, F., Giannakis, G.B.: 'Frequency offset and symbol timing recovery in flat fading channel: a cyclostationary approach', *IEEE Trans. Commun.*, 1998, **46**, (3), pp. 400–411
32 Simon, M.K., Divsalar, D.: 'Doppler corrected differential detection in MPSK', *IEEE Trans. Commun.*, 1989, **37**, (2), pp. 99–109
33 Mengali, U., Andrea, A.N.: 'Synchronization techniques for digital receivers' (Plenum Press, New York, 1997)
34 Mueller, K.H., Muller, M.: 'Timing recovery in digital synchronous data receivers', *IEEE Trans. Commun.*, 1976, **14**, pp. 516–530
35 Gardner, F.M.: 'A BPSK/QPSK timing error detector for sampled receivers', *IEEE Trans. Commun.*, 1986, **34**, pp. 423–429
36 Hyvarinen, A., Oja, E.: 'Independent component analysis: algorithms and applications', *Neural Netw.*, 2004, **13**, pp. 411–430
37 Cardoso, J.F., Souloumiac, A.: 'Jacobi angles for simultaneous diagonalization', *SIAM J. Matrix Anal. Appl.*, 1996, **17**, (1), pp. 161–164
38 Beres, E., Adve, R.: 'Blind channel estimation for orthogonal STBC in MISO systems', *IEEE Trans. Veh. Technol.*, 2007, **56**, (4), pp. 2042–2050
39 Kannan, A., Krauss, T.P., Zoltowski, M.D.: 'Separation of cochannel signals under imperfect timing and carrier synchronization', *IEEE Trans. Veh. Technol.*, 2001, **50**, (1), pp. 79–96
40 Abeysekera, S.S.: 'Efficient frequency estimation using the pulse-pair method at various lags', *IEEE Trans. Commun.*, 2006, **54**, (9), pp. 1542–1546
41 Serpedin, E., Chevreuil, A., Giannakis, G.B., Loubaton, P.: 'Blind channel and carrier frequency offset estimation using periodic modulation precoders', *IEEE Trans. Signal Process.*, 2000, **48**, (8), pp. 2389–2405
42 Morelli, M., Mengali, U.: 'Carrier frequency estimation for transmissions over selective channels', *IEEE Trans. Commun.*, 2000, **48**, (9), pp. 1580–1589
43 Goldsmith, A.: 'Wireless communications' (Cambridge University Press, 2005)

© The Institution of Engineering and Technology 2011